

Silicon Detectors for Low Energy Particle Detection

C.S. Tindall, N.P. Palaio, B.A. Ludewigt, S.E. Holland

Lawrence Berkeley National Laboratory, Berkeley, CA 94720

D.E. Larson, D.W. Curtis, S.E. McBride, T. Moreau, R.P. Lin¹, V. Angelopoulos

Space Sciences Laboratory, University of California Berkeley, Berkeley, CA 94720-7450

¹Also Physics Department, University of California, Berkeley, CA 94720-7300

Abstract— Silicon detectors with very thin entrance contacts have been fabricated for use in the IMPACT SupraThermal Electron (STE) instrument on the STEREO mission and for the Solid State Telescopes on the THEMIS mission. The silicon diode detectors were fabricated using a 200Å thick phosphorous doped polysilicon layer that formed the thin entrance window. A 200 Å thick aluminum layer was deposited on top of the polysilicon in order to reduce their response to stray light. Energy loss in the entrance contact was about 350 eV for electrons and about 2.3 keV for protons. The highest detector yield was obtained using a process in which the thick polysilicon gettering layer was removed by chemical etching rather than chemical mechanical polishing.

Manuscript received November 15, 2006. This work was supported in part by NASA contracts NAS5-00133 for the IMPACT investigation on the STEREO mission, and NAS5-02099 for the THEMIS mission.

C.S. Tindall is with the Lawrence Berkeley National Laboratory, Berkeley, CA 94720 USA (telephone: 510-486-6523, e-mail: CSTindall@lbl.gov).

N.P. Palaio is with the Lawrence Berkeley National Laboratory, Berkeley, CA 94720 USA (telephone: 510-486-7177, e-mail: NPPalaio@lbl.gov).

B.A. Ludewigt is with the Lawrence Berkeley National Laboratory, Berkeley, CA 94720 USA (telephone: 510-486-7733, e-mail: Bernhard_Ludewigt@lbl.gov).

S.E. Holland is with the Lawrence Berkeley National Laboratory, Berkeley, CA 94720 USA (telephone: 510-486-5069, e-mail: SEHolland@lbl.gov).

D.E. Larson is with Space Sciences Laboratory, University of California, Berkeley, Berkeley, CA 94720 USA (telephone: 510-642-7558, e-mail: davin@ssl.berkeley.edu).

D.W. Curtis is with Space Sciences Laboratory, University of California, Berkeley, Berkeley, CA 94720 USA (telephone: 510-642-5998, e-mail: dwc@ssl.berkeley.edu).

S.E. McBride is with Space Sciences Laboratory, University of California, Berkeley, Berkeley, CA 94720 USA (telephone: 510-643-9782, e-mail: mcbride@ssl.berkeley.edu).

T. Moreau is with Space Sciences Laboratory, University of California, Berkeley, Berkeley, CA 94720 USA (telephone: 510-642-7558, e-mail: moreau@ssl.berkeley.edu).

R.P. Lin is with Space Sciences Laboratory, University of California, Berkeley, Berkeley, CA 94720 USA (telephone: 510-642-1149, e-mail: rlin@ssl.berkeley.edu).

V. Angelopoulos is with Space Sciences Laboratory, University of California, Berkeley, Berkeley, CA 94720 USA (telephone: 510-643-1871, e-mail: vassilis@ssl.berkeley.edu).

I. INTRODUCTION

The objective of this work was to fabricate silicon semiconductor diode detectors (SSDs) with very thin entrance contacts that may be used to detect low energy particles for space plasma physics measurements. In the past, silicon semiconductor detectors have primarily been used for measurements of electrons and ions with energies greater than ~20 to 30 keV because of the thickness of the detector contacts (also because of the high capacitance of the detectors used (areas $\gg 1\text{cm}^2$ and thickness ~ 300 microns). The electric field does not penetrate the contact fully and hence electron hole pairs created in this field free region have a significant probability of recombining before they can be collected. Incident particles that are not energetic enough to enter the active region of the device will not be detected. For silicon detectors with contacts that have been fabricated using standard ion implantation techniques, the junction depth has been reported to be about 3000Å [1], a window thickness corresponding to about a 30 keV threshold for protons (20 keV for electrons).

In the past, because of this limitation of silicon diode detectors, alternative methods of detecting particles with energies lower than 30 keV had to be employed. Windowless electron multiplier detectors (channeltrons and microchannel plates (MCPs)) have been used most often. However, they provide no information on the energy of the incident particles and thus bulky, electrostatic or magnetic analyzers are required to sort the particles according to their energy in a relatively slow, power consuming process. Silicon detectors, on the other hand, provide intrinsic energy resolution. The amount of charge collected is proportional to the initial energy of the incident particle since electron-hole pairs are created at the rate of one pair for every 3.6 eV of energy deposited in the active region of the device. A second disadvantage of MCPs and electrostatic analyzers is that they require high voltage power supplies (typically 2 to 3 kV or more) in contrast to silicon detectors that generally require 100V or less to operate. Third, electron multipliers often have significant gain and

efficiency drifts [2] whereas silicon detectors tend to be much more stable.[3]

Some of the advantages of SSDs versus the standard electrostatic analyzers for low energy (down to ~1-2 keV) electron detection can be illustrated by comparing the Electrostatic Analyzer (EESA-H) instrument successfully flown as part of UC Berkeley Space Sciences Lab's (SSL's) 3D Plasma and Energetic Particles (3DP) investigation on the Wind spacecraft[4] with the SSD-based SupraThermal Electron (STE) instrument[5] selected as part of the IMPACT instrument suite[6] for NASA's STEREO mission (planned launch October 2006). For example, the electron superhalo from >2 to ~ 100 keV was discovered by the high sensitivity electron measurements on WIND using EESA-H, a very large electrostatic analyzer (~ 20 cm diameter, ~ 3 kg, ~ 3 W), with anticoincidence rejection of the penetrating high energy particle background. However, because the count rate above ~ 2 keV at quiet times was dominated by intrinsic background counts (~ 30 c/s), weak impulsive electron events could not be detected, and long integration times and careful background subtraction were required for the measurement of the superhalo. Also, for EESA-H it took ~ 14 contiguous energy steps to cover 2-20 keV, corresponding to a duty cycle of $\sim 7\%$ at a given energy. On the other hand, the STE instrument will measure electrons down to 2 keV, using small, thin-window, passively cooled SSDs, which measure all energies simultaneously (100% duty cycle). The SSDs background rate is also much lower.

II. BACKGROUND

Back and front illuminated silicon diode detectors with thin entrance contacts can be fabricated using several different process technologies. Detectors having a junction thickness on the order of 300\AA can be fabricated by ion implantation at low energies through an SiO_2 layer. The material is then counter doped using an n-type implant to enhance the electric field near the entrance contact.[7,8] X-rays with energies as low as 150 eV have been detected using detectors fabricated with this process.[1] Diffusion has also been successfully used to make thin entrance window contacts. In this case, the built-in field due to the strong inversion layer that exists at the oxide-silicon interface on p-type material is exploited to create a recombination free region. This gives the device very high internal quantum efficiency.[9,10,11] We did not use either of these two techniques because of our concern that the high processing temperatures needed in the absence of a gettering layer might lead to increased leakage current.[12] Detectors that have contacts made using other techniques such as molecular beam epitaxy, molecular layer doping and gas immersion doping have also been reported and hold great promise for making ultra-thin contacts.[13,14,15,16] However, due to a lack of fabrication equipment and expense, these techniques were not pursued.

III. PROCESSING TECHNIQUE

The processing technique that was used employs a thick, doped polysilicon layer on the wafer backside to getter impurities during the high temperature processing steps. This helps to maintain the material resistivity at values greater than $10\text{ k}\Omega\text{-cm}$ throughout the process and minimizes the incorporation of deep levels within the active area of the device that lead to increased leakage current.[12] In order to form the thin contact, near the end of the process, the one micron thick gettering layer was removed either by chemical etching or chemical-mechanical polishing (CMP). A 100\AA to 200\AA thick, doped polysilicon layer was then deposited on the entrance side of the detectors to form the n+ contact.[17] For the STEREO mission the detection of electrons was desired. For the Time History of Events and Macroscale Interactions During Substorms (THEMIS) mission detection of both low energy electrons and ions was required. Although the telescopes are expected to be well shielded from stray light, a reduction in the detectors' sensitivity to light, as an additional pre-caution, was achieved by depositing a 100\AA to 200\AA thick layer of aluminum over the doped-poly silicon contact.

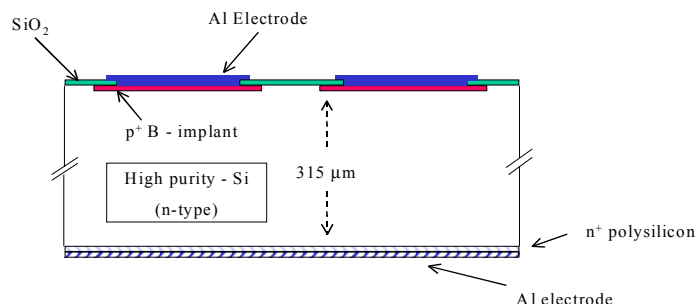


Fig. 1a – Cross-sectional view of detectors fabricated for this work.

The detector arrays were fabricated on $315\text{ }\mu\text{m}$ thick, high resistivity, $\langle 100 \rangle$ n-type silicon substrates. Fig. 1a shows the cross section of silicon diodes. The resistivity of the starting material was approximately $8,000\text{ }\Omega\text{-cm}$. For STE, the $3\text{ mm} \times 3\text{ mm}$ detector elements were arranged in a 1×4 linear array (figure 1b), with a multiple guard ring structure to gradually drop the bias voltage and to take up the surface leakage current. The innermost guard ring was grounded in order to ensure that there was no potential difference between the detector elements and the innermost guard ring. For the THEMIS detectors (figure 1c), the starting material was the same. Only the geometry of the detector was different. It consisted of a single large pixel of approximately 1 cm^2 surrounded by several smaller pixels and a multiple guard ring. The detectors were operated fully depleted, so that the electric field extended to the back contact.

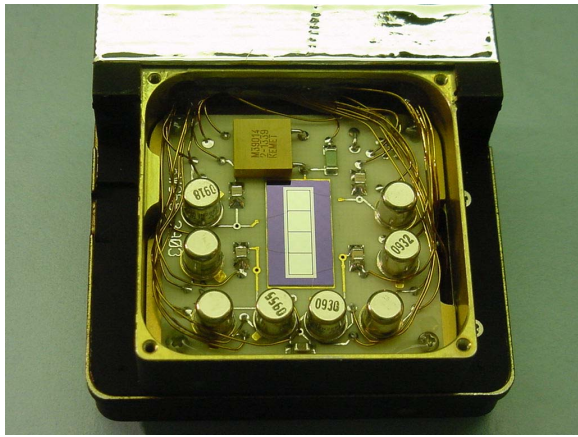


Fig. 1b – STE detector array, shown here mounted on the STE electronics board.

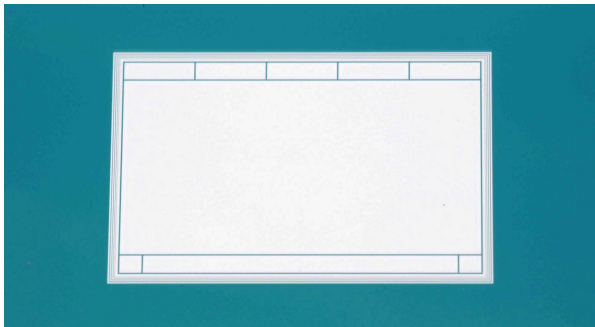


Figure 1c – Detector die used to make the Solid State Telescopes (SSTs) for the THEMIS mission. The center pixel has an area of 0.924 cm^2 .

IV. DETECTOR PROCESSING AND RESULTS

In order to determine the best method for fabricating the thin entrance contact, different processing steps were tested. The first set of variations involved the treatment of the silicon surface on which the contact was deposited, i.e. the unpatterned side of the wafer. The first two sets of wafers were polished on only one side, i.e. single side polished (SSP). The backside had been etched, but not polished, and the polysilicon gettering layer was deposited on this un-polished surface on which the thin contact was ultimately deposited. For the first group of wafers, after completion of all of the high temperature processing steps, the gettering layer was removed by CMP and the entrance contact side of the wafer was polished to a prime wafer finish. The thin, doped polysilicon contact was then deposited directly onto this polished surface. For the second group of wafers, the thick gettering layer was removed by chemical etching only. Finally, a third group of wafers was processed in which the starting material was polished on both sides to a prime finish, i.e. double side polished (DSP). As with the second group, the thick gettering layer was removed by chemical etching.

The treatment of the entrance contact surface had a significant effect on the performance and yield of the detectors. The overall yield of arrays in which all of the detection elements performed satisfactorily was about 35% for the group that had the gettering layer polished off. A detector

was considered to have satisfactory performance if the leakage current before dicing was less than 500 pA/cm^2 . All the detectors in this group were fabricated using the STE layout, with four (each with area = 9 mm^2) pixels per detector. The second group, in which the starting material was polished only on one side, and the gettering layer was removed using chemical etching only, had the highest yield of about 80% overall. On these detectors, a single element of area $\sim 1 \text{ cm}^2$ was tested. The third set, in which double side polished material was used from the beginning, had an overall yield of about 67% for the $\sim 1 \text{ cm}^2$ detectors. These results suggest that mechanical polishing of the backside has a detrimental effect on the performance of detectors with thin polysilicon contacts.

Additionally, two types of thin polysilicon contacts were fabricated, one consisting of a 100\AA doped polysilicon layer covered with a 100\AA layer of aluminum/1% silicon, and a second that consisted of a 200\AA polysilicon layer covered with a 200\AA metal layer. The aluminum on the patterned side of the wafer was sintered in forming gas at 400°C . However, the aluminum that was deposited over the polysilicon contact did not receive any heat treatment. Detectors without any metal layers on the polysilicon contact were also made and tested. All of the aforementioned detectors consisted of four 9 mm^2 pixels. Also, in this process, the thick gettering layer was removed using chemical mechanical polishing just prior to depositing the thin polysilicon contact layer. In this group of detectors, the best yield and performance was obtained from the thick poly without any metal deposition. The yield of the detectors with 100 \AA polysilicon / 100 \AA aluminum contact layers was very low. (See table 1) These yields were obtained by measuring the detector performance before dicing the wafers and thus do not include losses due to dicing or wirebonding.

V. DETECTOR TEST RESULTS

First detector tests were performed by measuring leakage current and capacitance as function of bias voltage. Fig. 2 shows the leakage current of a typical detector. For the detector with a total area of 0.924 cm^2 , the leakage current at 60V was 162 pA/cm^2 and at 100V reverse bias was 188 pA/cm^2 . This measurement was made after wire-bonding and mounting the detector in its flight holder. A typical capacitance vs. bias voltage measurement is shown in Fig. 3. This measurement was made on one of the test diodes on a STE wafer. The detector fully depletes by about 18 volts bias. Above full depletion, the capacitance levels off at about 3.3 pF . This is in reasonable agreement with the calculated bulk capacitance of 2.9 pF . The resistivity of the material was maintained at a level greater than $10 \text{ k}\Omega\text{-cm}$ throughout the fabrication process. The residual impurity level was found to be between $3 \cdot 10^{11}$ and $4 \cdot 10^{11} \text{ cm}^{-3}$.

In order to test detector performance and to measure the thickness of the entrance window, detectors (STE detector diodes, 9 mm^2 area, $315 \text{ }\mu\text{m}$ thick, figure 1b) were bombarded with both electrons and protons of known energies. The detection elements were wirebonded to the input low-noise FET of a charge-sensitive preamplifier similar to the prototype

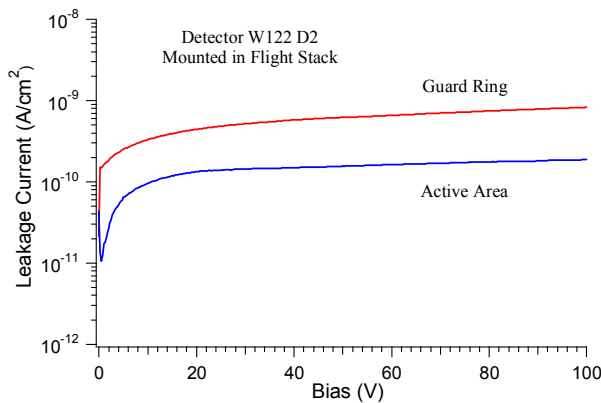


Fig. 2 – Leakage current vs. bias voltage at ambient temperature of a 0.924 cm² silicon PIN diode, 315 microns thick.

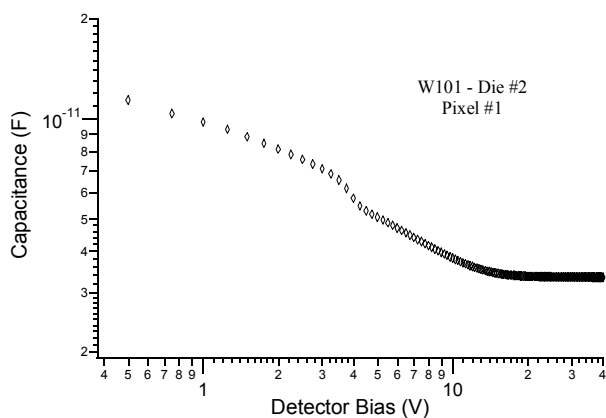


Figure 3 – Capacitance vs. bias of a STE pixel with a total area of 9 mm². This measurement was made at room temperature. Full depletion is attained at about 18 volts.

TABLE 1

| Group # | Starting Material | Gettering Layer Removal Method | Poly Contact / Al Thickness (Å) | Total Pixel Area (cm ²) | Yield (%) |
|---------|-------------------|--------------------------------|---------------------------------|-------------------------------------|-----------|
| 1 | SSP, etched | CMP | 100 / 100 | 0.36 | 22 |
| 2 | SSP, etched | CMP | 200 / 200 | 0.36 | 35 |
| 3 | SSP, etched | CMP | 200 / 0 | 0.36 | 61 |
| 4 | SSP, etched | Chemical Etching | 200 / 200 | 0.924 | 75 |
| 5 | SSP, etched | Chemical Etching | 200 / 0 | 0.924 | 81 |
| 6 | DSP | Chemical Etching | 200 / 0 | 0.924 | 67 |

mounting board for the STE sensor shown in figure 1b and connected to amplification, shaping and digitizing electronics. Figure 4a shows the result of measurements for electrons with energies as low as 3 keV. The detector was at ambient temperature. From the measured data one can estimate the energy lost in the window and therefore the thickness of the window from the y-intercept. For electrons, the energy lost is estimated to be about 350 eV. No bias dependence of the

window thickness was observed above full depletion. The result for protons with energies as low as 5.0 keV is shown in Figure 4b. For very low energies below 5 keV, the calculated range in silicon deviates from this simple straight-line approximation. However, in the energy range studied, a straight line gives a reasonably good approximation. For protons, the energy loss estimated in this way is approximately 2.3 keV. In further tests, threshold values for electrons of between 1.1 keV and 2.7 keV were observed at room temperature. The energy resolution measured with an ⁵⁵Fe source at 5.9 keV varied between 0.9 keV and 2.6 keV FWHM for the tested detector elements at ambient temperature. The detector bias during this test was 10 volts and the shaping time was 4 μs. In order to obtain the lowest possible noise, the field effect transistors (FETs) were pre-selected for low noise and uniformity. There was about 15% variation in the noise of the FETs used. The average noise was about 700 eV FWHM at room temperature. This is believed to be dominated by voltage noise because the FET leakage current was estimated to be less than 10 pA based on the reset rate of the preamp. For the best detectors, the noise at ambient temperature is dominated by electronic (FET) noise. However, for the detectors that exhibited lower resolution, a significant amount of noise is contributed by the detector leakage current at room temperature. These detectors were fabricated using the process that employed CMP to remove the gettering layer and thus exhibited more variability in leakage current than did

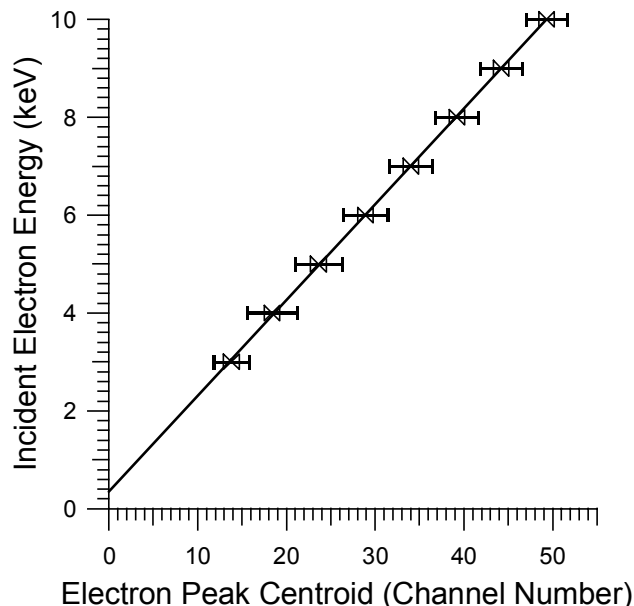


Figure 4a - Laboratory measurements of electrons down to 3 keV. The detector was a 3mm x 3mm, 300 micron thick SSD for the STE sensor. The error bars show the FWHM of the measured peak. The measurements were taken at ambient temperature. The polysilicon layer was 200Å underneath a 100Å layer of aluminum.

those made using the optimized process. For lower temperature operation (<-40°C), the FET noise dominates.

A typical spectrum taken using the STE detectors is shown in Figure 5. This spectrum was taken at ambient temperature. The detector bias was 80V and the shaping time was again 4 μ s. The detector was exposed to an ^{55}Fe and a ^{109}Cd source simultaneously. All of the anticipated X-ray lines associated with the two sources are observed and are labeled in the figure.

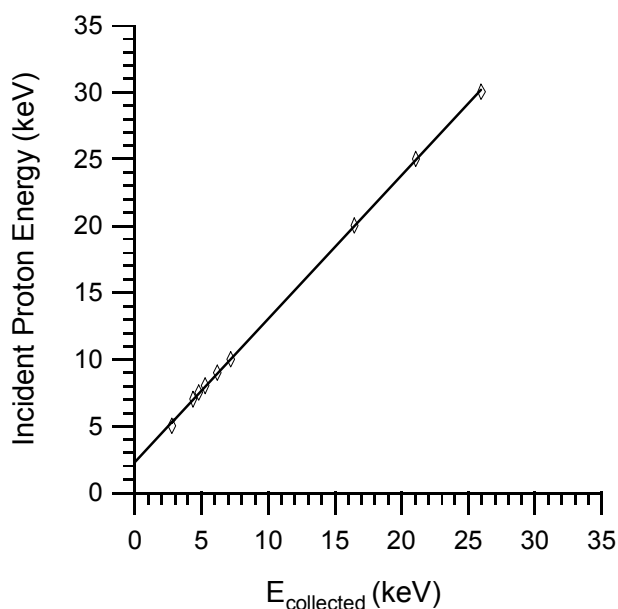


Figure 4b - Laboratory measurements of protons down to 5.0 keV. The detector was a 3mm x 3mm, 300 micron thick SSD for the STE sensor. The detector temperature was 77K. The polysilicon layer was 200 \AA underneath a 100 \AA layer of aluminum.

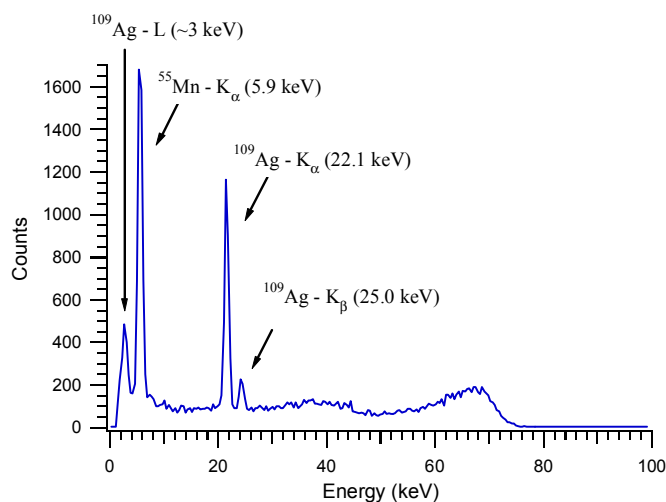


Figure 5 - Spectrum obtained by illuminated a STE detector with a source of one μCi ^{55}Fe and a one μCi ^{109}Cd simultaneously. This spectrum was acquired at ambient temperature. The detector bias was 80V and the shaping time was 4 μ s. The broad peaks at about 68 keV and 38 keV are due to conversion electrons from the ^{109}Cd source, the energy of which has been reduced by their passage through a thin plastic cover over the source and several millimeters of air.

For example, the ^{55}Mn K_{α} X-ray at 5.9 keV is the largest peak in the spectrum. The counting time was too short to observe the 88 keV gamma ray associated with the ^{109}Cd decay because the branching ratio for the gamma ray is only about 3.6% and the photoelectric cross-section of silicon is low at this high energy. The broad peaks centered around 68 keV and 38 keV and the higher background at energies below 78 keV is due to conversion electrons produced by ^{109}Cd source. The initial energies of these conversion electrons are 84 keV and 62 keV. However, the energy of these electrons is reduced by their passage through a 15 μm thick plastic cover on the source as well as several millimeters of air.

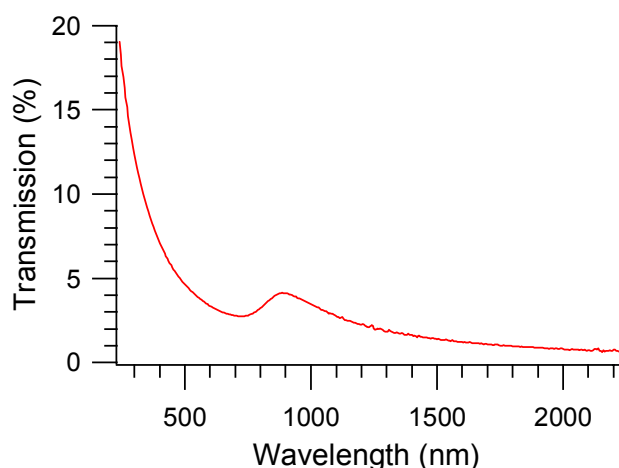


Figure 6 - Measured transmission of a 200 \AA thick layer of Aluminum / 1% silicon alloy sputtered onto a quartz wafer.

Finally, since the reduction in sensitivity of the detectors to stray light is an important requirement for this application, the light sensitivity was reduced by sputtering a thin (200 \AA) layer of aluminum alloyed with 1% silicon onto the entrance contact of the detectors. The optical transmission of an identical aluminum/silicon alloy thin film was measured by sputtering it onto a quartz wafer. The optical transmission as a function of wavelength corrected for the transmission of quartz is shown in figure 6. The measured transmission is somewhat higher than, but agrees qualitatively with expectations from known reflectance and the extinction coefficients of bulk aluminum at wavelengths longer than about 700nm.[18,19] Increased optical transmission is expected given that the film is not pure aluminum and because it is so thin it likely contains pinholes. Alloying aluminum with other metals, for example 0.5% iron reduces its reflectivity significantly.[20] Moreover, the film will oxidize in air which should also reduce its reflectance and absorption.[21] Below 700nm, the measured optical transmittance increases sharply. This is in contrast to what is expected based on the bulk properties of aluminum. The plasma frequency of bulk aluminum, above which one would expect to see a sharp rise in the optical transmission, resides at a much shorter wavelength, about 82 nm. The origin of this apparent increase in the transmission is not clear at present. It is possible that the plasma frequency of the film shifts down

somewhat due to the presence of silicon in the film.[22,23] Also, the micro-structure of the film may influence the transmission spectrum.[24]

Detectors both with and without any metal film were placed in a light tight box and illuminated with a group of ten red light emitting diodes (LEDs). Figure 7 shows the leakage current vs. LED current for a detector with and another without metal. The 200Å thick layer of metal reduces the photocurrent by factor of about 14. This is in reasonable agreement with the measured transmission of the film at that wavelength. The inner most guard ring was not grounded during this measurement.

VI. CONCLUSION

We have fabricated silicon particle detectors with very thin entrance contacts. These detectors are particularly useful for space applications because they are much lighter, more compact and use far less power than the electrostatic analyzers coupled with microchannel plates that have been used for this energy range in the past. They are also capable of collecting data more quickly since the signal pulse height is directly related to the energy of incoming particle. This eliminates the need for energy analyzers and provides essentially 100% duty cycle at all energies.

The detectors we have fabricated have an energy threshold for electrons of about 1.1 keV and an energy resolution of between 0.9 keV and 2.1 keV FWHM at ambient temperature. Cooling to the STE lowest design temperature of approximately -90°C improved the energy resolution to about 700 eV FWHM. The energy lost in the entrance contact is about 350 eV. In a separate measurement, spectra of protons with energies as low as 5.0 keV were obtained at 77K. The energy loss in the window was estimated to be about 2.3 keV.

The light sensitivity of the detectors was reduced by depositing a layer of aluminum alloyed with 1% silicon on top of the thin polysilicon contact. In the case of the THEMIS detectors, measurements showed that the light was attenuated by about a factor of 14 in the red portion of the spectrum by a 200Å thick aluminum film.

REFERENCES

- [1] R. Hartmann, et al., "Low energy response of silicon pn-junction detector", Nucl. Instrum. Methods in Physics Research, **A377**, 191-196, 1996.
- [2] M.V. Zombeck, L.P. David, F.R. Harnden Jr., and K.M. Kearns, "Orbital performance of the high-resolution imager (HRI) on ROSAT", Proceedings of SPIE -- Volume 2518, EUV, X-Ray, and Gamma-Ray Instrumentation for Astronomy VI, Oswald H. W. Siegmund, John V. Vallerga, Editors, September 1995, pp. 304-321.
- [3] Gerhard Lutz, Semiconductor Radiation Detectors: Device Physics, Springer, 1999.
- [4] R.P. Lin, et al., A three-dimensional (3-D) plasma and energetic particle experiment for the WIND spacecraft of the ISTP/GGS mission. *Space Sci. Rev.* **71**, 125 (1995).
- [5] R. P. Lin, et al., The IMPACT SupraThermal Electron (STE) Instrument. *Space Sci. Rev.* in preparation, (2006).
- [6] J. G. Luhmann, et al., STEREO IMPACT Investigation Overview. *Space Sci. Rev.* in preparation, (2006).

- [7] T. Maisch, et al, "Ion-Implanted Si pn-Junction Detectors with Ultrathin Windows", Nucl. Instrum. Methods in Physics Research, **A288**, 19-23, 1990.
- [8] S. Hillert, et al, "Test Results on the Silicon Pixel Detector for the TTF-FEL Beam Trajectory Monitor", Nucl. Instrum. Methods in Physics Research, **A458**, 710-724, 2001.
- [9] Raj Korde and Jon Geist, "Stable, High Quantum Efficiency, UV-Enhanced Silicon Photodiodes by Arsenic Diffusion", Solid State Electronics, **30**, 89-92, 1987.
- [10] Raj Korde and Jon Geist, "Quantum efficiency stability of silicon photodiodes", Appl. Optics, **26**, 5284-5290, 1987.
- [11] K. W. Wenzel, "Soft X-Ray Silicon Photodiodes with 100% Quantum Efficiency", IEEE Trans. Nucl. Sci., **41**, 979-983, 1994.
- [12] Steve Holland, "Fabrication of Detectors and Transistors on High-Resistivity Silicon", Nucl. Instrum. Methods in Physics Research, **A275**, 537-541, 1989.
- [13] M.E. Hoenk, et al, "Growth of a delta-doped silicon layer by molecular beam epitaxy on a charge-coupled device for reflection-limited ultraviolet quantum efficiency", Appl. Phys. Lett., **61**, 1084-1086, 1992.
- [14] Y. Saitoh et al, "New profiled silicon PIN photodiode for scintillation detection", IEEE Trans. Nucl. Sci., **42**, 345-350, 1995.
- [15] P.G. Carey, K. Bezjian, T.W. Sigmon, P. Gildea and T.J. Magee, "Fabrication of submicrometer MOSFET's using gas immersion laser doping (GILD)", IEEE Elec. Dev. Lett., **7**, 440-442, 1986.
- [16] S. Nikzad, et. al., "Direct Detection of 0.1-20 keV electrons with delta doped, fully depleted, high purity silicon p-i-n diode arrays", Appl. Phys. Lett., in press.
- [17] S.E. Holland, N.W. Wang and W.W. Moses, "Development of Low Noise, Back-Side Illuminated Silicon Photodiode Arrays", IEEE Trans. Nucl. Sci., **44**, 443-447, 1997.
- [18] J.H. Weaver, "Optical Properties of Metals", Physics Data, Nr. 18-1 and 18-2, 74-79.
- [19] E. Shiles, Taizo Sasaki, Mitio Inokuti and D.Y. Smith, "Self-consistency and sum-rule tests in the Kramers-Kronig analysis of optical data: Applications to aluminum, Phys. Rev. B, **22**, 1612-1628, 1980.
- [20] G. Hass, W.R. Hunter and R. Tousey, "Influence of Purity, Substrate Temperature, and Aging Conditions on the Extreme Ultraviolet Reflectance of Evaporated Aluminum", J. Opt. Soc. America, **47**, 1070-1073, 1957.
- [21] R.W. Fane and W.E.J. Neal, "Optical Constants of Aluminum Films Related to the Vacuum Environment", J. Opt. Soc. America, **60**, 790-793, 1970.
- [22] H. Ibach and D.L. Mills, Electron Energy Loss Spectroscopy and Surface Vibrations, New York : Academic Press, 1982.
- [23] C. Kittel, Introduction to Solid State Physics, New York : John Wiley, 2005.
- [24] O. Stenzel, A. Stendal, M. Röder and C. von Borczyskowski, "Tuning of the Plasmon Absorption Frequency of Silver and Indium Nanoparticles Via Thin Amorphous Silicon Films", Pure Appl Opt, **6**, 577-588 (1997).